A Geometrical-based 3D Model for Fixed MIMO BS-RS Channels

Wei Chen, Jianhua Zhang, Zhenzi Liu, and Yuming Bi
Key Lab of Universal Wireless Communications, Ministry of Education
Beijing University of Posts and Telecommunications, Beijing, 100876, P.R. China
✉ Emails: chenweiw09@gmail.com, {jhzhang, liuzhenzibupt}@bupt.edu.cn, biyuming10507@sina.com.

***Abstract*—This work proposes a three-dimensional (3D) reference model for multiple-input multiple-output (MIMO) base station to relay station (BS2RS) Rician fading channels. First, the new stochastic reference model, based on the geometrical one-sphere model, is obtained under the assumption that both base station and relay station are stationary while an infinite number of local scatterers around the RS move in random directions. Then, the closed-form spatial and temporal correlation functions between each two sub-channels are derived in the 3D non-isotropic scattering environment, and a detailed discussion is also made to demonstrate their properties. Finally, we find that our proposed channel model can cover several communication scenarios (e.g., fixed-to-mobile (F2M) and fixed-to-fixed (F2F) scenarios, etc.), and make a detailed simulation to illustrate the property of our proposed model.**

***Index Terms*—MIMO, Rician fading, closed-form, 3D non-isotropic scattering**

I. Introduction

Relay architectures have been identified as a key tool of the 4G wireless cellular communication networks in providing robustness against channel variations, extending the coverage, and improving energy efficiency [1]. The relevant definition and channel modelling of the relay station (RS) have been introduced in release 9 of the 3GPP Long Term Evolution (LTE) standards [2]. However, this channel model does not take the temporal variations into account when both the BS and RS are stationary. It is in [3] pointing out that the channel temporal variations can be caused by scatterers motion in a fixed wireless channel and undoubtedly, the variations will be further enhanced in high-frequency communications. Therefore, accurate channel models, which sufficiently approximate the temporal and spatial correlation properties of fixed multiple-input multiple-output (MIMO) BS2RS channels, are really required.

In a typical macrocell, the BS is elevated and receives the signal within a narrow beam-width, whereas the receiver is surrounded by local scatterers. MIMO channel modelling of this typical macrocell environment has been investigated for such a long time. Among them, one of the most popular channel models is the geometrical channel model with a ring of scatters around the receiver or around the transmitter [4]. It has been extended in [5] and [6], where a rich isotropic distribution of scatters is assumed around the mobile station (MS) and wideband MIMO channel models are proposed. Other models, such as two-ring models and ellipse models [7] [8], have also been proposed to model the special shape of scattering region. A multiple-ring cooperative MIMO channel model was proposed [9] and the BS2RS link spatial correlation are numerically analyzed. In [10], a three-dimension (3D) two-sphere model was proposed for the case where scattered waves may not necessarily travel horizontally and the authors in [11] developed a 3D macrocell model to jointly analyze the spatial and temporal domain. Additionally, in [12] the authors analyzed the space-time correlated function of 3D mobile relay fading channels.

The use of MIMO radio channels is an effective means to profit from the temporal and spatial diversity. Therefore, ignoring the variation of Doppler shifts in the fixed MIMO relay networks makes no sense. For fixed wireless communication applications, the received signals still experience Doppler shifts even if the subscriber and the transmitter are stationary [13]. This phenomenon was studied in [14], where time variations arose from mobile scatterers, e.g., wind-blown foliage, pedestrians and vehicles, and a corresponding channel model was proposed. Then, a further study of different speed scattering model is proposed in [3]. To the best of our knowledge, the effects of moving scatterers in MIMO relay channel modeling have NOT been investigated, which motivates us to make a further research on this topic, and publish our work.

The main contribution of our work can be summarized as follows:

- proposing a new 3D channel model for the fixed BS2RS channels based on the one-sphere model
- deriving closed-form spatial and temporal cross-correlation functions (CCF) for 3D non-isotropic scattering environment

The rest of the paper is organized as follows: In Section II, system geometries are described briefly and the complex channel gains associate with the new 3D reference models are presented. Section III presents the derivation of the closed-form space-time correlation function for 3D non-isotropic scattering. In Section IV, simulation results are made and discussed in detail. Finally, Section V concludes the paper.

II. Three-Dimension Reference Model for MIMO Relay Channels

This paper, for ease of analysis, considers a narrowband MIMO relay communication system with N_T transmit and N_R receive omnidirectional antenna elements. The radio propagation environment between the the transmitter T_x (i.e., BS) and the receiver R_x (i.e., RS) is characterized by 3D non-isotropic scattering with both Line-Of-Sight (LOS) and None Line-Of-Sight (NLOS) conditions. Fig. 1 illustrates our model with $N_R = N_T = 2$ antenna elements where local scatterers of the RS are modeled

978-1-4673-6782-0/15/$31.00 ©2015 IEEE

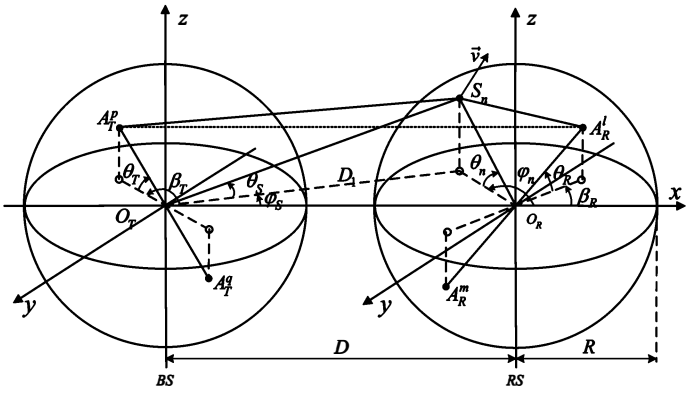

Fig. 1. The proposed three-dimensional local scatter model for R_x in condition of 2×2 MIMO channel.

on the surface of a sphere of radius R. In fact, the main difference between our proposed model and the other existing models [10]–[12] lies in the consideration of both *randomly moving scatterers*, denoted by $s_n (n = 1, 2, \ldots)$, and the *simplified assumption of single-bounce and direct rays* due to the characteristics of relay links. Herein, δ_T, δ_R, φ_n, θ_n, φ_s and θ_s indicate the antenna element spacing at T_x, antenna element spacing at R_x, main Azimuth Angle of Arrival (AAOA) of the nth scatterer, main Elevation Angle of Arrival (EAOA) of the nth scatterer, auxiliary Azimuth Angle of Departure (AAOD), auxiliary Elevation Angle of Departure (EAOD), respectively. While β_T, β_R, θ_T and θ_R denote the orientation of T_x with reference to x-axis, orientation of R_x with reference to x-axis, elevation of T_x with reference to the x-y plane, and the elevation of T_x with reference to the x-y plane, respectively.

It is worth noting that the distance D is assumed much larger than the radius R, (i.e., $R \ll D$), and only local scatterers are considered in this paper due to the high path loss property of remote scatterers.

Considering the scenario that single-bounce rays over s_n are received at R_x and LOS paths may exist between any pair of BS-RS antenna elements, the complex channel gain $h_{lp}(t)$ expressed in (1) is introduced to describe the time-variant property of the link between the pth transmit antenna element A_T^p and the lth receive antenna element A_R^l, i.e., $A_T^p - A_R^l$, in the frequency flat MIMO channel.

$$h_{lp}(t) = h_{lp}^{LOS}(t) + h_{lp}^{NLOS}(t) \tag{1}$$

where $h_{lp}^{LOS}(t)$ and $h_{lp}^{NLOS}(t)$ denote the complex channel gain with LOS propagation conditions and NLOS propagation conditions, respectively, and can be written by

$$h_{lp}^{LOS}(t) = \frac{1}{\sqrt{K_{lp}+1}} \exp\left\{-\frac{j2\pi}{\lambda} d_{pl}\right\} \tag{2}$$

where K_{lp} is the Rice factor of the link A_T^p to A_R^l, which is defined as the ratio of the LOS component power to the diffuse component power, and d_{pl} denotes the distance between A_T^p and A_R^l. Note that according to the statistical properties of the channel described above, the model reduces to a MIMO Rayleigh fading channel when $K_{lp} = 0$.

$$h_{lp}^{NLOS}(t) = \frac{1}{\sqrt{K_{lp}+1}} \lim_{N\to\infty} \frac{1}{\sqrt{N}} \cdot \sum_{n=1}^{N} \exp\left\{j\Psi_n - \frac{j2\pi}{\lambda}(d_{ps_n} + d_{ls_n}) + j2\pi f_n t\right\} \tag{3}$$

where N is the number of scatterers and Ψ_n ($n = 1, 2, \ldots, N$), associated phase shifts introduced by the scatterer s_n, is generally assumed a independent and identically distributed (i.i.d) random variable with uniform distributions over $[0, 2\pi]$, while d_{ps_n}, d_{ls_n}, λ and f_n represent the distance between A_T^p and s_n, distance between A_R^l and s_n, wavelength and frequency caused by scatterers moving, respectively, and f_n is expressed as the following

$$\begin{aligned} f_n &= f_{b-s} + f_{r-s} \\ &= \frac{v}{\lambda}\left[\cos\theta_n \cos(\alpha_n - \varphi_n) + \cos\theta_s \cos(\alpha_n - \varphi_s)\right] \end{aligned} \tag{4}$$

where f_{b-s} and f_{r-s} are the Doppler shift caused by scatterer motion with respect to the BS and to the RS, respectively. v denotes the velocity of s_n, and α_n represents the moving direction of s_n distributed uniformly over $[0, 2\pi]$.

III. Space-time cross-correlation function of the three-dimensional reference model

In this section we will derive the space-time CCF of the complex channel gains described in (2) and (3).

Considering two sub-channels $A_T^p - A_R^l$ and $A_T^q - A_R^m$, the normalized space-time CCF between them is defined by $\rho_{lp,mq}(\tau) = E\left[h_{lp}(t) h_{mq}^*(t+\tau)\right]$, where $(\cdot)^*$ denotes complex conjugate operation and $E[\cdot]$ is the statistical expectation operation. Interestingly, if we further define $\rho_{lp,mq}^{LOS}(\tau) = E\left[h_{lp}^{LOS}(t) h_{mq}^{LOS*}(t+\tau)\right]$ and $\rho_{lp,mq}^{NLOS}(\tau) = E\left[h_{lp}^{NLOS}(t) h_{mq}^{NLOS*}(t+\tau)\right]$, then the normalized space-time CCF can be simplified as $\rho_{lp,mq}(\tau) = \rho_{lp,mq}^{NLOS}(\tau) + \rho_{lp,mq}^{LOS}(\tau)$ [15]. Moreover, the empirical observations of $D \gg R \gg \max\{\delta_R, \delta_T\}$ justify the simple but useful approximate results for both $\rho_{lp,mq}^{NLOS}(\tau)$ and $\rho_{lp,mq}^{LOS}(\tau)$. In the following sections III-A and III-B, we will derive the accurate and approximate expressions for LOS and NLOS parts of the normalized space-time CCF.

A. Cross-correlation Function of the NLOS Component

Based on the properties of Ψ_n and equation (3), the space-time CCF between sub-channel gains $h_{lp}^{NLOS}(t)$ and $h_{mq}^{NLOS}(t)$ can be rewritten as

$$\begin{aligned} \rho_{lp,mq}^{NLOS}(\delta,\tau) = &\frac{1}{\sqrt{(K_{lp}+1)(K_{mq}+1)}} \lim_{N\to\infty} \frac{1}{N} \sum_{n=1}^{N} \\ &\exp\left\{-\frac{j2\pi}{\lambda}(d_{ps_n} - d_{qs_n} + d_{ls_n} - d_{ms_n}) - j2\pi f_n t\right\} \end{aligned} \tag{5}$$

where d_{qs_n} and d_{ms_n} denote the distance between A_T^q and s_n and the distance between A_R^m and s_n, while similarly, K_{mq} represents the Rice factor of the sub-channel $A_T^q - A_R^m$.

For those large values of N, the discrete φ_n and θ_n can be replaced by continuous random variables φ and θ with joint probability density function (PDF) $p(\varphi, \theta)$, while the discrete α_n can be replaced by α with the PDF $p(\alpha)$. Furthermore, assume that the azimuth and elevation angles are independent of each other, and then the joint

PDF $p(\varphi,\theta)$ can be decomposed to $p(\varphi)p(\theta)$. Hence, (5) can be further reduced to the following integral form

$$\rho_{lp,mq}^{NLOS}(\delta,\tau)=\frac{1}{\sqrt{(K_{lp}+1)(K_{mq}+1)}}\int_{\alpha}\int_{\theta}\int_{\varphi}\exp\left\{-\frac{j2\pi}{\lambda}\cdot\right.$$
$$\left.(d_{ps_n}-d_{qs_n}+d_{ls_n}-d_{ms_n})-j2\pi f_n t\right\}p(\varphi)p(\theta)p(\alpha)d\varphi d\theta d\alpha \quad (6)$$

For given $p(\varphi)$ and $p(\theta)$, (6) needs to be calculated numerically. According to the law of cosines in appropriate triangles and the assumption $\max\{\delta_T,\delta_R\}\ll R$, we can obtain the following approximations

$$d_{ps_n}-d_{qs_n}\approx$$
$$-\delta_T^{pq}\left[\cos\theta_T\cos\theta_s\cos(\beta_T-\varphi_s)+\sin\right. \quad (7)$$

$$d_{ls_n}-d_{ms_n}\approx$$
$$-\delta_R^{lm}\left[\cos\theta_R\cos\theta_n\cos(\beta_R-\varphi_n)+\sin\theta_R\right.$$

Furthermore, considering the fact that for many practical cases of interest, the angle spread $\Delta=\arcsin(R/$ at the BS is generally small for macrocells in urban, most often less than 15° [16]. Based on the previous assumption $D\gg R$, we have $D_1\approx D$ and $R/D_1\approx\Delta$. Together with sin approximations are obtained

$$\begin{cases}\varphi_s\approx\Delta\cos\theta_n\sin\varphi\\ \cos(\beta_T-\varphi_s)\approx\cos\beta_T+\Delta\sin\end{cases} \quad (9)$$

Consequently, (6) can be rewritten as

$$\rho_{lp,mq}^{NLOS}(\delta,\tau)\approx\frac{1}{\sqrt{(K_{lp}+1)(K_{mq}+1)}}\cdot$$
$$\int_{\alpha}\int_{\theta}\int_{\varphi}e^{j\Theta}p(\varphi)p(\theta)p(\alpha)d\varphi d\theta d\alpha \quad (10)$$

Here,

$$\Theta = \frac{2\pi}{\lambda}\left(\delta_{Tx}^{pq}+\Delta\delta_T^{pq}\sin\right.$$
$$+\frac{2\pi\delta_R^{lm}}{\lambda}\left[\sin\right.$$
$$-\frac{2\pi v\tau}{\lambda}\left[\cos\theta\cos(\alpha-\varphi)+\cos\alpha\right]$$

where $\delta_{Tx}^{pq}=\delta_T^{pq}\cos\theta_T\cos\beta_T$, $\delta_{Ty}^{pq}=\delta_T^{pq}\cos\theta_T\sin$ $\delta_{Rx}^{lm}=\delta_R^{lm}\cos\theta_R\cos\beta_R$, and $\delta_{Ry}^{lm}=\delta_R^{lm}\cos\theta_R\sin\beta_R$.

As mentioned before, the variable α is uniformly distributed over $[0,2\pi)$ and is independent of φ. Then, (10) can be further expressed as

$$\rho_{lp,mq}^{NLOS}(\delta,\tau)\approx\frac{I_0\left(\frac{j2v\pi}{\lambda}\tau\right)}{I_0(\kappa)\sqrt{(K_{lp}+1)(K_{mq}+1)}}\cdot$$
$$\int_{\theta}\int_{\varphi}I_0\left(\frac{j2v\pi}{\lambda}\tau\cos\theta\right)e^{j\Omega}p(\theta)p(\varphi)d\varphi d\theta \quad (11)$$

Here,

$$\Omega = \frac{2\pi}{\lambda}\left(\delta_{Tx}^{pq}+\Delta\delta_T^{pq}\sin\right.$$
$$+\frac{2\pi\delta_R^{lm}}{\lambda}\left[\sin\right.$$

Several different scatterer distributions, such as uniform, Gaussian, and Laplacian, have been explored in prior works to characterize the azimuth variables φ. In this paper, the von Mises PDF [17] is applied, because it approximates many of the previously mentioned distributions and leads to closed-form solutions for many useful situations. The space-time CCF then can be given by

$$\rho_{lp,mq}^{NLOS}(\delta,\tau)\approx\frac{I_0\left(\frac{j2v\pi}{\lambda}\tau\right)}{I_0(\kappa)\sqrt{(K_{lp}+1)(K_{mq}+1)}}\cdot$$
$$\int_{\theta}\exp\left\{\frac{j2\pi}{\lambda}\delta_{Tx}^{pq}\right\}I_0\left(\sqrt{z^2+w^2}\cos\theta\right)$$
$$I_0\left(\frac{j2v\pi}{\lambda}\tau\cos\theta\right)\exp\left\{j\zeta\sin\theta\right\}p(\theta) \quad (12)$$

where $z=\frac{j2\pi}{\lambda}\left(\Delta\delta_{Ty}^{pq}+\delta_{Ry}^{lm}\right)+\frac{\kappa\sin u}{\cos\theta}$, $w=\frac{j2\pi}{\lambda}\delta_{Rx}^{lm}+\frac{\kappa\cos u}{\cos\theta}$, $\zeta=\frac{2\pi}{\lambda}\left(\Delta\delta_T^{pq}\sin\theta_T\right.$ order modified Bessel function, $u\in[-\pi,\pi)$ accounts for the mean direction of AAOA in $x-y$ plane and κ controls the spread of AAOA.

In fact, since the LOS component is deterministic, the temporal auto-correlation function (ACF) only depends on the NLOS part. Therefore, the spatial and temporal variations can be considered separately. By setting $\delta_T=\delta_R=0$ in (12), the temporal ACF will be

$$\rho_{ACF}(\tau)=\frac{J_0^2(\frac{v}{\lambda}\pi\tau)J_0\left(\frac{2v\pi}{\lambda}\tau\right)}{\sqrt{(K_{lp}+1)(K_{mq}+1)}} \quad (13)$$

(13) demonstrates that all scatterers move randomly at exact speed v, which may be overly pessimistic. Actually, the speeds of the scatterers follow a certain distribution, e.g., $p(v_0)$, in real scenarios. Therefore, the ACF becomes a function of delay, namely $\rho_{ACF}(\tau)=\int_{v_0}\frac{J_0^2(\pi\tau\frac{v_0}{\lambda})J_0\left(2\pi\tau\frac{v_0}{\lambda}\right)}{\sqrt{(K_{lp}+1)(K_{mq}+1)}}p(v_0)dv_0$. More details could be found in [3].

In order to characterize the continuous random variables θ, we assume that the elevation angle distribution function is a uniform distribution over $[-\pi/2,\pi/2]$. Substitution of $\tau=0$ into (12), the spatial CCF can be written as

$$\rho_{CCF}^{NLOS}(\delta) \approx \frac{\exp\left\{\frac{j2\pi}{\lambda}\delta_{Tx}^{pq}\right\}}{\pi I_0(\kappa)\sqrt{(K_{lp}+1)(K_{mq}+1)}}\int_{-\frac{\pi}{2}}^{\frac{\pi}{2}}$$
$$I_0\left(\sqrt{z^2+w^2}\cos\theta\right)\exp\left\{j\zeta\sin\theta\right\}$$

Moreover, apply the computing techniques described in [18](e.q. 6.688), then the closed-formed expression of spatial CCF can be finally given by

$$\rho_{CCF}^{NLOS}(\delta) \approx \frac{J_0\left(\frac{\sqrt{z_1^2+w_1^2+\zeta^2}-\zeta}{2}\right)J_0\left(\frac{\sqrt{z_1^2+w_1^2+\zeta^2}+\zeta}{2}\right)}{I_0(\kappa)\sqrt{(K_{lp}+1)(K_{mq}+1)}}\cdot$$
$$\exp\left\{\frac{j2\pi}{\lambda}\delta_{Tx}^{pq}\right\} \quad (15)$$

where $w_1=\frac{2\pi}{\lambda}\delta_{Rx}^{lm}-j\kappa\cos u$ and $z_1=\frac{2\pi}{\lambda}\left(\Delta\delta_{Ty}^{pq}+\delta_{Ry}^{lm}\right)-j\kappa\sin$

B. Cross-correlation function of the LOS component

The space-time CCF between $h_{lp}^{LOS}(t)$ and $h_{mq}^{LOS}(t)$ in terms of LOS part is

$$\rho_{lp,mq}^{LOS}(\tau)=\sqrt{\frac{K_{lp}K_{mq}}{(K_{lp}+1)(K_{mq}+1)}}\exp\left\{-\frac{j2\pi}{\lambda}(d_{lp}-d_{mq})\right\} \quad (16)$$

As shown in Fig.1, applying the law of cosines, then we can get

$$\begin{cases} d_{lp}^2 = \left(D - \frac{\delta_T^{pq}\cos\theta_T\cos\beta_T}{2} - \frac{\delta_R^{lm}\cos\theta_R\cos\beta_R}{2}\right)^2 \\ \qquad + \left(\frac{\delta_T^{pq}}{2}\sin\theta_T - \frac{\delta_R^{lm}}{2}\sin\theta_R\right)^2 \\ d_{mq}^2 = \left(D + \frac{\delta_T^{pq}\cos\theta_T\cos\beta_T}{2} + \frac{\delta_R^{lm}\cos\theta_R\cos\beta_R}{2}\right)^2 \\ \qquad + \left(\frac{\delta_T^{pq}}{2}\sin\theta_T - \frac{\delta_R^{lm}}{2}\sin\theta_R\right)^2 \end{cases} \quad (17)$$

Since $D \gg \delta_T$ and $D \gg \delta_R$, the complex expression of $d_{lp} - d_{mq}$ can be simplified as

$$\begin{aligned} d_{lp} - d_{mq} &\approx -(\delta_T^{pq}\cos\theta_T\cos\beta_T + \delta_R^{lm}\cos\theta_R\cos\beta_R) \\ &\approx -(\delta_{Tx}^{pq} + \delta_{Rx}^{lm}) \end{aligned} \quad (18)$$

Finally, the space-time CCF in terms of LOS part can be expressed as

$$\rho_{lp,mq}^{LOS}(\tau) = \sqrt{\frac{K_{lp}K_{mq}}{(K_{lp}+1)(K_{mq}+1)}}\exp\left\{\frac{j2\pi}{\lambda}\left(\delta_{Tx}^{pq} + \delta_{Rx}^{lm}\right)\right\} \quad (19)$$

To sum up, finally we obtain the closed-form CCF and ACF of our proposed 3D reference model. Deduced from our results, several existing F2M and F2F communications correlation functions can be obtained by simplifying our 3D MIMO relay channel space-time CCF. For example, the fixed outdoor channel temporal correlation function $J_0^2(2\pi f_{max}\tau)$ in [14] can be obtained from (12) by setting $K_{lp} = K_{mq} = 0$, $\delta_T = \delta_R = 0$ and $\theta = 0$. For 2D isotropic scattering, the spatial correlation function for MIMO F2M channels $J_0(2\pi d_R/\lambda)$ can be obtained from (14) with $K_{lp} = K_{mq} = 0$, $\delta_T = 0$, $\kappa = 0$, $\theta = 0$ and $\tau = 0$. Similarly, for 2D distribution of scatterers ($\theta = 0$), our reference model reduces to F2F communication channel model [3]. Expressions for other temporal correlation functions based on one-ring model can also be simply obtained with (12).

IV. Simulation Results

In this section, simulation results have been made to illustrate the performance of our proposed 3D reference model. Herein, the angles of the BS and RS antenna array used to obtain the curves are $\beta_T = \pi/4$, $\theta_T = \pi/3$, $\beta_R = \pi/4$, $\theta_R = \pi/2$ and the angle AAOA is assumed as $u = \pi$ and $\kappa = 1.2$. Furthermore, the identical maximum Doppler frequency, f_{max}, is assumed as 10Hz and the wave length λ is set to 0.15m. In addition, the angle spread Δ at BS and the Rice factors are set to 0.1 and $K_{lp} = K_{mq} = 2.55 = 4$dB, respectively.

Fig. 2 shows the ACF of the channels in the presence of moving scatterers. For comparison, the black line marked with circles corresponds to the Jakes model. The blue line represents the time correlation when all reflectors move exactly at the speed $v_{max} = 1.5$m/s. The red-dash line shows a more complex case where the scatterers move with velocity distributed uniformly over $[0, v_{max}]$. Clearly, the ACF of the proposed model drops with time and is different from the conventional Jakes model. Moreover, it is overly pessimisitc to assume that all scatterers move at exact speed v and we can see the blue line has a more rapid envelope decorrelation than the red-dash line.

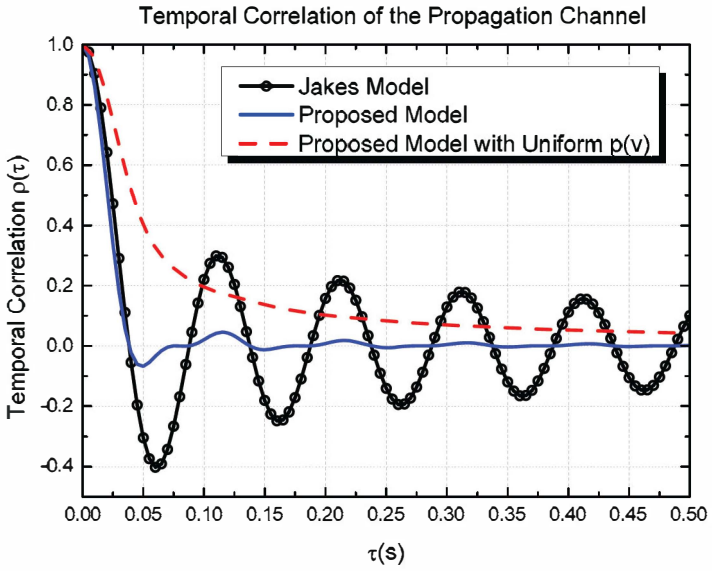

Fig. 2. The temporal correlation of the channels for different models.

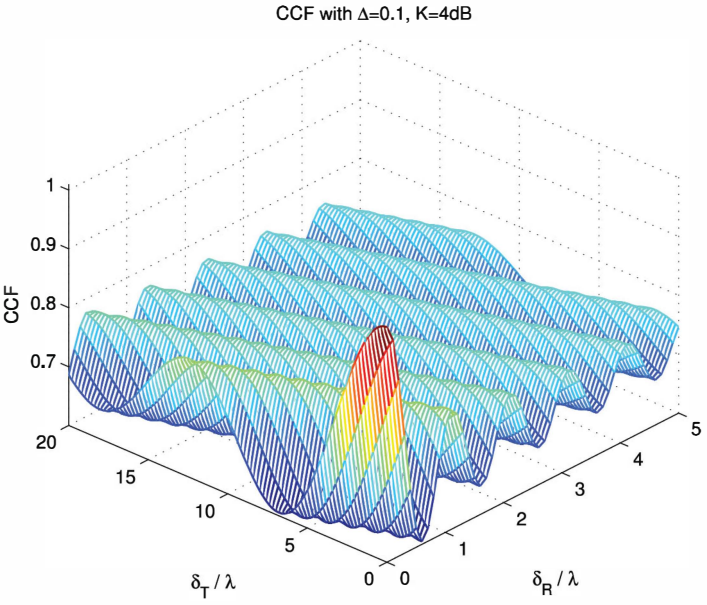

Fig. 3. The space correlation function of our proposed reference model.

Fig. 3 investigates the space correlation function of the reference model. To illustrate the validity of the approximate space correlation function in (15), we compare it with the numerical results in (14). Fig. 4 shows the CCF discrepancy between (14) and (15). It is shown that there is still a relatively small discrepancy between the numerical results and the approximate results, however, this error shows a nearly equiripple behavior, where the maximum values are smaller than 0.08. More importantly, this discrepancy decreases with decreasing κ and when κ is zero, there would be no discrepancy anymore. In a word, the approximations have a good match with the numerical results and can be a reference in system design and performance analysis.

In Fig. 5, we can see that the transmitter antenna correlation at the BS fall faster when the angle spread Δ is 10° than that when Δ is 5°. It is also can be seen that, the BS CCF obtained by our model has almost the same fluctuations comparing with the reference spatial CCF in [19], but our model has a smaller amplitude

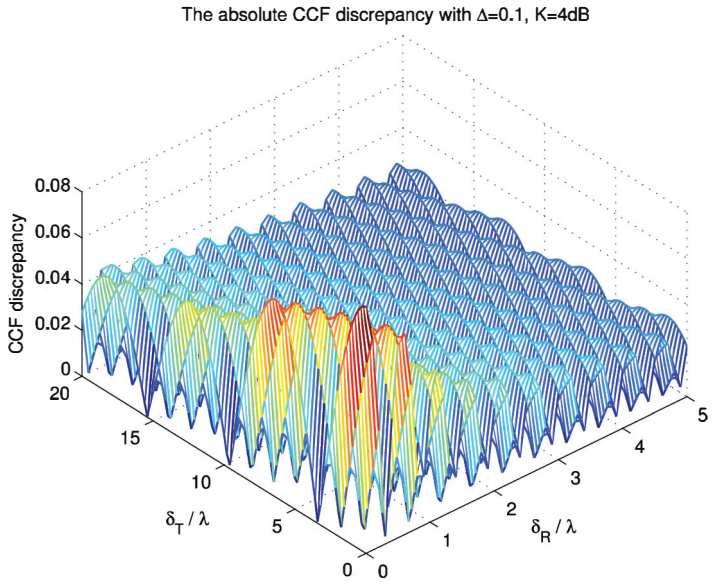

Fig. 4. The discrepancy between the numerical and approximate results.

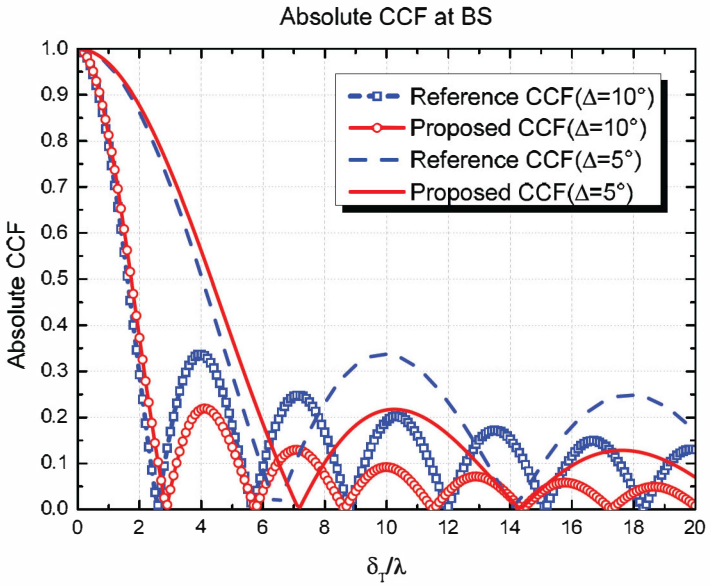

Fig. 5. The temporal auto-correlation function for the channel model with $K_{lp} = K_{mq} = 0$.

of fluctation because of considering the elevation angle information.

V. Concluding Remarks

This paper proposed a new theoretical 3D geometrical scattering reference model for multiple-input multiple-output (MIMO) base station to relay station (BS2RS) backhaul channels. Based on this geometrical model, both the closed-form spatial correlation function and the temporal correlation function between each two sub-channels for 3D non-isotropic scattering have been derived in detail. Furthermore, theoretical analysis demonstrate that some other channel models, e.g., 2D F2M, 2D F2F, etc, can be obtained by simplifying our model. In addition, both the impact of moving scatterers on the Doppler shift and the effects of antenna spacing on spatial correlation are also discussed. Finally, simulation results demonstrate the good performance of our proposed reference model.

VI. Acknowledgement

The work is supported by National Key Technology Research and Development Program of the Ministry of Science and Technology of China with NO. 2012BAF14B01, by National Science and Technology Major Project of the Ministry of Science and Technology with NO. 2013ZX03003009-002, and by the National Natural Science Foundation of China with NO. 61322110 and No. 61171105.

References

[1] K. P. Peppas, G. C. Alexandropoulos, and P. T. Mathiopoulos, "Performance analysis of dual-hop AF relaying systems over mixed and fading channels," *IEEE Trans. Veh. Tech.*, vol. 62, no. 7, pp. 3149 – 3163, 2013.

[2] E. U. T. R. Access, "Further advance-ments for E-UTRA physical layer aspects," 3GPP TR 36.814, Tech. Rep., 2010. [Online]. Available: www.3gpp.org

[3] V.-H. Pham, M. H. Taieb, J.-Y. Chouinard, S. Roy, and H.-T. Huynh, "On the double Doppler effect generated by scatterer motion," *REV J. Elec. Commun.*, vol. 1, no. 1, pp. 30 – 37, 2011.

[4] D.-S. Shiu, G. J. Foschini, M. J. Gans, and J. M. Kahn, "Fading correlation and its effect on the capacity of multielement antenna systems," *IEEE Trans. Commun.*, vol. 48, no. 3, pp. 502 – 513, 2000.

[5] M. Patzold and B. O. Hogstad, "A wideband space-time MIMO channel simulator based on the geometrical one-ring model," in *IEEE Conf. Veh. Tech.*, 2006, pp. 1 – 6.

[6] W. Hakimi, M. Ammar, A. Bouallegue, and S. Saoudi, "A generalised wideband space-time MIMO channel simulator based on the geometrical multi-radii one-ring model," in *IEEE Conf. Veh. Tech.*, 2008, pp. 1266 – 1270.

[7] X. Cheng, C.-X. Wang, and et al., "An adaptive geometry-based stochastic model for non-isotropic mimo mobile-to-mobile channels," *IEEE Trans. Wireless Commun.*, vol. 8, no. 9, pp. 4824–4835, 2009.

[8] M. M. Zadeh-Parizi Fatemeh and A.-S. Javad, "A survey of geometrically-based MIMO propagation channel models," 2013.

[9] X. Cheng, C.-X. Wang, and et al., "Cooperative MIMO channel modeling and multi-link spatial correlation properties," *IEEE J. Sel. Areas Commun.*, vol. 30, no. 2, pp. 388 – 396, 2012.

[10] X. Cheng, C.-X. Wang, Y. Yuan, D. I. Laurenson, and X. Ge, "A novel 3D regular-shaped geometry-based stochastic model for non-isotropic MIMO mobile-to-mobile channels." in *IEEE Conf. Veh. Tech.*, 2010, pp. 1 – 5.

[11] S. J. Nawaz, B. H. Qureshi, and N. M. Khan, "A generalized 3-D scattering model for a macrocell environment with a directional antenna at the BS," *IEEE Trans. Veh. Tech.*, vol. 59, no. 7, pp. 3193 – 3204, 2010.

[12] E. T. Michailidis, P. Theofilakos, and A. G. Kanatas, "A 3-D model for MIMO mobile-to-mobile amplify-and-forward relay fading channels," in *6th European Conf. Antennas and Propagation (EUCAP)*, 2012, pp. 2073 – 2077.

[13] S. Roy, H. T. Huynh, and P. Fortier, "Compound Doppler spread effects of subscriber motion and scatterer motion," *AEU - Int'l J. Elec. Commun.*, vol. 57, no. 4, pp. 237 – 246, 2003.

[14] P. Karadimas, E. D. Vagenas, and S. A. Kotsopoulos, "On the scatterers' mobility and second order statistics of narrowband fixed outdoor wireless channels," *IEEE Trans. Wireless Commun.*, vol. 9, no. 7, pp. 2119 – 2124, 2010.

[15] M. Dohler and Y. Li, *Cooperative communications: hardware, channel and PHY*. John Wiley & Sons, 2010.

[16] W. C. Lee, "Effects on correlation between two mobile radio base-station antennas," *IEEE Trans. Commun.*, vol. 20, no. 11, pp. 1214 – 1224, 1973.

[17] J. A. B. Abdi Ali and M. Kaveh, "A parametric model for the distribution of the angle of arrival and the associated correlation function and power spectrum at the mobile station," *IEEE Trans. Veh. Tech.*, vol. 51, pp. 425 – 433, May 2002.

[18] D. Zwillinger, *Table of integrals, series, and products*. Elsevier, 2014.

[19] C.-X. Wang, X. Hong, H. Wu, and W. Xu, "Spatial-temporal correlation properties of the 3GPP spatial channel model and the kronecker MIMO channel model," *EURASIP J. Wireless Commun. and Networking*, vol. 2007, no. 1, pp. 59–59, 2007.